

Superconducting and topological properties of compound $\text{Lu}_4\text{H}_7\text{N}$

Zheng-Wei Liao,¹ Xin-Wei Yi,¹ Jing-Yang You,^{2,*} Bo Gu,^{3,†} and Gang Su^{1,3,‡}

¹*School of Physical Sciences, University of Chinese Academy of Sciences, Beijing 100049, China*

²*Department of Physics, National University of Singapore, 2 Science Drive 3, Singapore 117551*

³*Kavli Institute for Theoretical Sciences, and CAS Center for Excellence in Topological Quantum Computation, University of Chinese Academy of Sciences, Beijing 100190, China*

A recent experiment has reported a nitrogen-doped lutetium hydride achieving a remarkable T_c of 294 K at just 1 GPa, significantly reducing the required pressure for obtaining room temperature superconductivity. However, subsequent experimental and theoretical investigations have encountered difficulties in replicating these results, leaving the structure of this Lu-H-N compound shrouded in uncertainty. Here, we propose a stable structure for $\text{Lu}_4\text{H}_7\text{N}$ employing first-principles calculations. Our calculations reveal that $\text{Lu}_4\text{H}_7\text{N}$ has a T_c of 1.044 K, which can be substantially enhanced to 11.721 K at 150 GPa, due to the increasing electron-phonon coupling (EPC). Notably, we delve into the nontrivial Z_2 band topology of $\text{Lu}_4\text{H}_7\text{N}$, featuring discernible surface states near the Fermi level, and we explore its spin Hall conductivity characteristics. Furthermore, we find that the electron doping can enhance the EPC strength and T_c of $\text{Lu}_4\text{H}_7\text{N}$, such as the $\text{Lu}_4\text{H}_7\text{O}$ structure we predict simulating electron doping for $\text{Lu}_4\text{H}_7\text{N}$ with an impressive T_c of 3.837 K. This work demonstrates the coexistence of superconducting and topological properties in a Lu-H-N system compound, which holds the promise of guiding the search for novel topological superconducting materials.

I. INTRODUCTION

Superconducting materials hold immense promise and practical applications across diverse fields, including energy, transportation, and healthcare, thanks to their excellent properties of zero electrical resistance and perfect diamagnetism. Nonetheless, the vast majority of superconductors exhibit disappointingly low superconducting temperatures (T_c), limiting their utility in real-world scenarios. Hence, the search for superconducting materials with substantially higher T_c , ideally at or near room-temperature, has been a longstanding aspiration [1]. During the final two decades of the preceding century, a pivotal breakthrough occurred with the discovery of copper-based superconductors capable of achieving T_c in the range of liquid nitrogen temperatures under ambient pressure with a record-high T_c of 130 K reported for the $\text{HgBa}_2\text{Ca}_2\text{Cu}_3\text{O}_{8+x}$ structure [2]. According to the tenets of BCS theory, attaining high T_c necessitates a high Debye temperature, which, in turn, demands high vibrational frequency and low atomic mass [3]. Naturally, hydrogen, characterized by its minuscule atomic mass, emerged as the focus of attention. However, a significant challenge arose from hydrogen's gaseous nature in standard environmental conditions, requiring extreme external pressures to induce metallic behavior. In 2004, Ashcroft proposed that the introduction of other elements surrounding hydrogen atoms can create a chemical pre-compressing environment that could reduce the external pressure required for hydrogen's metallization, which may facilitate the development of high T_c superconductors [4]. Since then, many hydrogen-rich materi-

als with high T_c have been predicted, including sulfur hydrides [5, 6], rare earth hydrides [7–9], alkali metal hydrides [10], alkali earth metal hydrides [11], and transition metal hydrides [12]. Among them, the LaH_{10} structure has been synthesized with the highest T_c , reaching 250–260 K at 170–190 GPa, remarkably close to room-temperature [8, 13]. However, it is evident that despite the impressive progress in enhancing the T_c of hydride superconductors, the critical challenge remains the exceptionally high pressure conditions required, imposing severe limitations on the practical applications of these materials. Therefore, the pursuit of methods to reduce the necessary pressure has emerged as a vital research direction in the realm of hydride superconductors.

Recently, Dasenbrock-Gammon *et al.* claimed that they discovered a Lu-H-N system achieving a T_c of 294 K at a low pressure of 1 GPa, much lower than the pressures required for H_3S and LaH_{10} [14]. This groundbreaking finding has sparked substantial interest in the Lu-H-N system as a potential avenue for high-temperature superconductivity. Their hypothesis revolves around the possibility of this compound adopting a $\text{Lu}_4\text{H}_{11}\text{N}$ structure, wherein a nitrogen atom replaces the hydrogen atom in either octahedral or tetrahedral interstitial sites of the $Fm\bar{3}m$ LuH_3 lattice. Unfortunately, many attempts to synthesize Lu-H-N compounds in experiments have not yielded T_c above 1.5 K within the pressure range from ambient to 50.5 GPa [17–27]. In addition, numerous theoretical works have sought to explore various Lu-H-N structures and elucidate the reasons behind the observed color changes in Lu-H-N compounds during experiments [28–37], but the precise structure remains elusive.

In this article, we found that the $\text{Lu}_4\text{H}_{11}\text{N}$ structures by replacing the octahedral or tetrahedral interstitial H atom with a N atom respectively and even $Fm\bar{3}m$ LuH_3 are dynamically unstable. Therefore, we used CALYPSO [38] to search Lu-H-N compounds with radii of

* phyjyy@nus.edu.sg

† gubo@ucas.ac.cn

‡ gsu@ucas.ac.cn

Lu:H:N from 4:7:1 to 4:4:4, and obtained a new stable structure $\text{Lu}_4\text{H}_7\text{N}$ with a space group of $C2/m$ with a Tc of 1.044 K and EPC λ of 0.413. By electron doping or applying pressure, the Tc of $\text{Lu}_4\text{H}_7\text{N}$ can be enhanced. The Tc of $\text{Lu}_4\text{H}_7\text{O}$, which is electron doped relative to $\text{Lu}_4\text{H}_7\text{N}$, reaches 3.837 K, and at a pressure of 150 GPa, $\text{Lu}_4\text{H}_7\text{N}$ exhibits a higher Tc of 11.721 K. Notably, $\text{Lu}_4\text{H}_7\text{N}$ features robust topological properties, including a strong Z_2 index and clear surface states near the Fermi level. The spin Hall conductivity (SHC) of $\text{Lu}_4\text{H}_7\text{N}$ is evaluated to be about $55\sim 145 \hbar \cdot (e \cdot \Omega \cdot \text{cm})^{-1}$ at the Fermi level, with the potential to soar to $292 \hbar \cdot (e \cdot \Omega \cdot \text{cm})^{-1}$ at 0.47 eV.

II. CALCULATION METHOD

The first-principles calculations were based on the density-functional theory (DFT) as implemented in the Vienna *ab initio* (VASP) [39], *Wannier90* [40], *WannierTools* [41], and QUANTUM-ESPRESSO (QE) packages [42], with the projector augmented wave method [43]. VASP was used to optimize the structure until the forces on atoms are less than $1\text{meV}/\text{\AA}$, and to calculate the electronic band structure, within the Perdew-Burke-Ernzerhof parameterization of the generalized gradient approximation [44]. The plane-wave cutoff energy was taken as 500 eV. The Monkhorst-Pack scheme was used to sample the Brillouin zone with a k-mesh of $9 \times 9 \times 9$.

Wannier90 and *Wanniertools* packages were used to obtain the effective tight-binding Hamiltonian, SHC, surface spectra and topological properties. SHC tensor is calculated by employing the Kubo formula [45, 46]:

$$\sigma_{\alpha\beta}^{\gamma} = e\hbar \int \frac{dk}{(2\pi)^3} \Omega_{\alpha\beta}^{\gamma}(k), \quad (1)$$

where $\Omega_{\alpha\beta}^{\gamma}(k)$ is the k-resolved term obtained by integrating the spin Berry curvature $\Omega_{n,\alpha\beta}^{\gamma}(k)$ of all occupied bands. The k-point mesh for the spin Berry curvature integral adopts $100 \times 100 \times 100$, and an extra $5 \times 5 \times 5$ fine mesh around those points with $\Omega_{n,\alpha\beta}^{\gamma}(k)$ exceeding 100\AA^2 is added. Spin-orbit coupling (SOC) is considered in SHC calculation.

The calculations of phonon spectra and superconducting properties were performed using QE within density functional perturbation theory (DFPT) [47]. The plane-waves kinetic-energy cutoff was set as 90 Ry and the q-point mesh in the first BZ was taken as $4 \times 4 \times 4$. An unshifted k-point mesh of $16 \times 16 \times 16$ was utilized. In the DFPT calculations, Methfessel-paxton smearing method [48] with a smearing value 0.010 Ry was taken. To estimate Tc, we use the McMillan-Allen-Dynes equation [49, 50]:

$$\text{Tc} = \frac{\omega_{log}}{1.2} \exp\left[-\frac{1.04(1+\lambda)}{\lambda - \mu^*(1+0.62\lambda)}\right], \quad (2)$$

where ω_{log} is the logarithmically averaged phonon frequency, and λ is a dimensionless parameter describing the EPC strength. The effective screened Coulomb repulsion constant μ^* was taken as a typical value of 0.1.

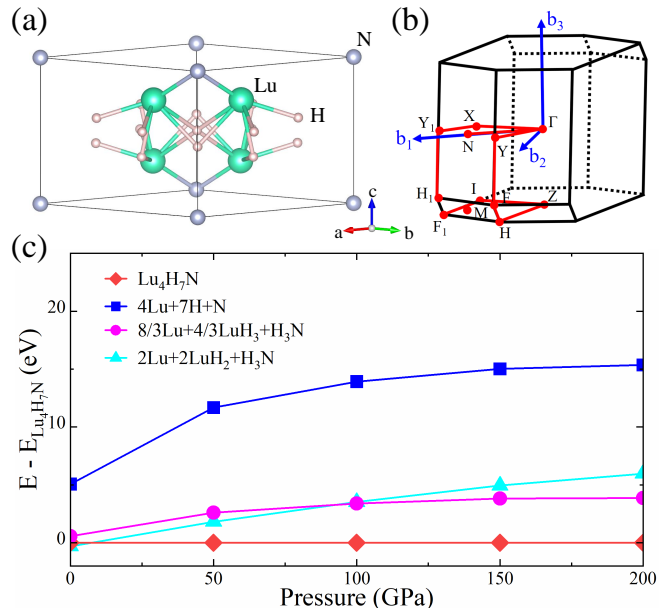


FIG. 1. (a) The crystal structure, (b) Brillouin zone (BZ), and (c) formation enthalpy of $\text{Lu}_4\text{H}_7\text{N}$.

III. RESULTS

A. Crystal structure and stability of $\text{Lu}_4\text{H}_7\text{N}$

Given the prevailing ambiguity surrounding the structural configuration of the Lu-H-N system, we adopted an approach by replacing the hydrogen atom in octahedral and tetrahedral interstitial sites of $Fm\bar{3}m$ LuH_3 with a nitrogen atom as suggested by Dasenbrock-Gammon *et al.*, respectively [14]. However, upon conducting thorough calculations, we observed that the phonon spectra for these two structures have imaginary frequencies, indicative of dynamic instability. Notably, even LuH_3 also displays imaginary phonons (detailed analysis is given in Sec. S1 of the Supplemental Materials [51]). Therefore, we focus our exploration on the well-established and stable $Fm\bar{3}m$ LuH_2 structure. Employing CALYPSO, we conducted an extensive search for potential structures, varying the Lu:H:N ratio from 4:7:1 to 4:4:4, and obtained a dynamically stable structure $\text{Lu}_4\text{H}_7\text{N}$ with a $C2/m$ space group as depicted in Fig.1(a). The optimized lattice constants are $a = 6.224 \text{\AA}$ and $c = 5.555 \text{\AA}$ with lattice angles of $\alpha = 91.739^\circ$ and $\gamma = 141.526^\circ$. In Fig.1(b), we present the Brillouin zone, highlighting the high-symmetry paths $\Gamma\text{-Y-F-H-Z-I-F}_1|\text{H}_1\text{-Y-X-}\Gamma\text{-N|M-}\Gamma$. In Fig.1(c), we determined the formation en-

thalpies of $\text{Lu}_4\text{H}_7\text{N}$ at different pressures to compare with those of multiple synthesis pathways using some synthesized structures, such as Lu ($P6_3/mmc$), H_2 ($P6_3/mmc$), N_2 ($Pa\bar{3}$), LuH_3 ($P\bar{3}c1$), LuH_2 ($Fm\bar{3}m$), LuN ($Fm\bar{3}m$), and H_3N ($P2_13$). It can be seen that $\text{Lu}_4\text{H}_7\text{N}$ boasts a lower energy. Furthermore, it's noteworthy that the formation energy of Lu_2N_3 , a compound synthesized experimentally with a space group of $Ia\bar{3}$, stands at 0.86 eV/atom above the hull [52, 53]. This value is notably higher than the formation energy of $\text{Lu}_4\text{H}_7\text{N}$ at ambient pressure, which registers at 0.43 eV/atom. Thus, it is possible to obtain this $\text{Lu}_4\text{H}_7\text{N}$ structure in experiment.

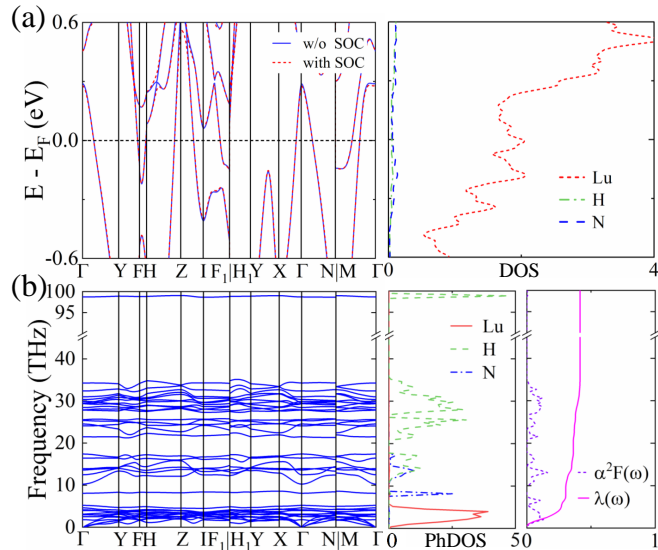


FIG. 2. (a) The electronic band structure, projected density of states (DOS) without and with spin-orbit coupling (SOC), (b) phonon spectrum, projected phonon density of states (PhDOS), Eliashberg spectral function $\alpha^2F(\omega)$, and cumulative frequency-dependent EPC $\lambda(\omega)$ of $\text{Lu}_4\text{H}_7\text{N}$.

B. Superconductivity of $\text{Lu}_4\text{H}_7\text{N}$

Through the first-principles calculations, we find that the T_c of $\text{Lu}_4\text{H}_7\text{N}$ is 1.044 K with the EPC λ 0.413. Fig.2(a) gives the electronic band structures and projected density of states (DOS) for $\text{Lu}_4\text{H}_7\text{N}$ without and with SOC, revealing its metallic nature. In particular, Lu atoms contribute to the majority of DOS near the Fermi level. In Fig.2(b), the phonon spectra, projected phonon density of states (PhDOS), Eliashberg spectral function $\alpha^2F(\omega)$, and cumulative frequency-dependent EPC $\lambda(\omega)$ of $\text{Lu}_4\text{H}_7\text{N}$ are comprehensively analyzed. It's evident that vibration modes below 5 THz predominantly originate from Lu atoms, while a distinct flat band around 8THz results from the vibration of N atoms. On the other hand, H atoms play a substantial role in contributing vibration modes higher than 10 THz. Remarkably, the low-frequency vibration region below 10 THz accounts for

about 73% of the total EPC, underscoring the pivotal significance of Lu and N atoms as the principal contributors to the EPC in $\text{Lu}_4\text{H}_7\text{N}$.

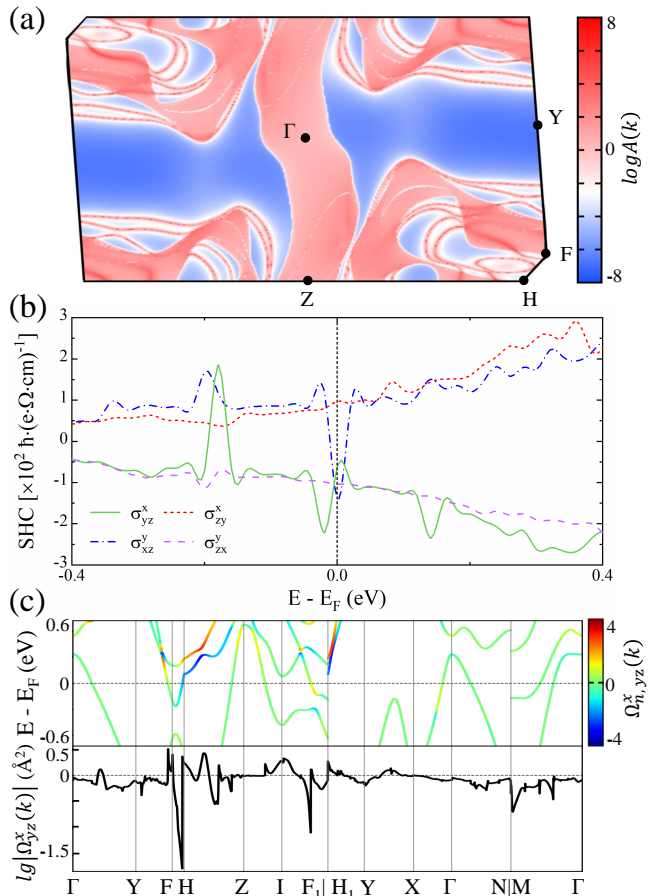


FIG. 3. (a) The isoenergy slice at 0.2 eV of the surface state spectrum $A(\mathbf{k}, \omega)$ projected along [010] direction, (b) four larger independent components of spin Hall conductivity (SHC) tensor as a function of chemical potential, (c) band structure weighted by spin Berry curvature $\Omega_{n,zy}^x(\mathbf{k})$ and \mathbf{k} -resolved $\Omega_{n,zy}^x(\mathbf{k})$ by integrating the spin Berry curvature of all occupied bands along the high-symmetry paths at the Fermi level for $\text{Lu}_4\text{H}_7\text{N}$.

C. Topological properties of $\text{Lu}_4\text{H}_7\text{N}$

Topological superconductivity is a promising method for quantum computing, so the quest for materials exhibiting both superconducting and topological properties has become a focal point of intense interest [54–56]. As shown in Fig. 2(a), several band gapped points emerge along the H - Z - I paths at around 0.2~0.5 eV close to the Fermi level because of SOC. To delve deeper into the topological properties, we calculated the Z_2 index, yielding a result of (1,001), a clear indication that $\text{Lu}_4\text{H}_7\text{N}$ qualifies as a topological semimetal [57]. Considering the

presence of a mirror symmetry within the $C2/m$ space group, we examined the mirror plane (010) of $\text{Lu}_4\text{H}_7\text{N}$. Fig. 3(c) illustrates an isoenergy slice at 0.2 eV for the surface state spectrum $A(\mathbf{k}, \omega)$ projected along the [010] direction, which clearly outlines the surface states.

We further investigate the SHC of $\text{Lu}_4\text{H}_7\text{N}$ from the intrinsic contribution, an intrinsic property contingent upon the electronic band structure and topological characteristics. The crystal symmetry of $\text{Lu}_4\text{H}_7\text{N}$ imposes constraints on the SHC tensor, encompassing thirteen independent components [58]. We have calculated these thirteen independent components and displayed the four most substantial components σ_{yz}^x , σ_{zy}^x , σ_{xz}^y , and σ_{zx}^y in Fig. 3(b). The components exhibit magnitudes in the range of $55\sim 145 \hbar \cdot (e \cdot \Omega \cdot \text{cm})^{-1}$ at the Fermi level, with σ_{zy}^x notably reaching an impressive $292 \hbar \cdot (e \cdot \Omega \cdot \text{cm})^{-1}$ at 0.47 eV. To reveal the nature of SHC, we plot the band structure of $\text{Lu}_4\text{H}_7\text{N}$ colored by the magnitude of spin Berry curvature $\Omega_{n,yz}^x(\mathbf{k})$, as well as the \mathbf{k} -resolved Ω_{yz}^x at the Fermi level in Fig. 3(c). It is obvious that $\Omega_{n,yz}^x(\mathbf{k})$ shows conspicuous peaks aligning with positions of small gapped points, signifying their primary contributions to SHC [59].

TABLE I. The DOS at the Fermi level $N(E_F)$ (in unit of states/spin/eV/cell), volume of primitive cell V (\AA^3), ω_{log} (K), λ , and T_c (K) for $\text{Lu}_4\text{H}_7\text{N}$ at ambient pressure, 10, 100, 150, and 200 GPa.

$P(\text{GPa})$	$N(E_F)$	$V(\text{\AA}^3)$	$\omega_{log}(\text{K})$	λ	$T_c(\text{K})$
0	18.53	134.13	207.3	0.413	1.044
10	17.88	120.12	213.0	0.464	1.892
100	13.10	77.28	214.5	0.724	8.097
150	12.18	69.31	219.4	0.860	11.721
200	11.66	64.09	237.4	0.773	10.355

TABLE II. The DOS at Fermi level $N(E_F)$ (in unit of states/spin/eV/cell), volume of primitive cell V (\AA^3), ω_{log} (K), λ , and T_c (K) for $\text{Lu}_4\text{H}_7\text{N}$, LuH_2 , $\text{Lu}_4\text{H}_7\text{C}$ and $\text{Lu}_4\text{H}_7\text{O}$ at ambient pressure.

	$N(E_F)$	$V(\text{\AA}^3)$	$\omega_{log}(\text{K})$	λ	$T_c(\text{K})$
$\text{Lu}_4\text{H}_7\text{N}$	18.53	134.13	207.3	0.413	1.044
LuH_2	3.95	31.67	297.4	0.258	0.024
$\text{Lu}_4\text{H}_7\text{C}$	8.32	136.88	232.6	0.235	0.059
$\text{Lu}_4\text{H}_7\text{O}$	20.89	134.81	149.7	0.624	3.837

D. Discussion

To gain a deeper insight into the superconducting properties of $\text{Lu}_4\text{H}_7\text{N}$, we conducted calculations in two aspects. First, we applied pressure to $\text{Lu}_4\text{H}_7\text{N}$ and found that upon reaching a pressure of 10 GPa, the structure

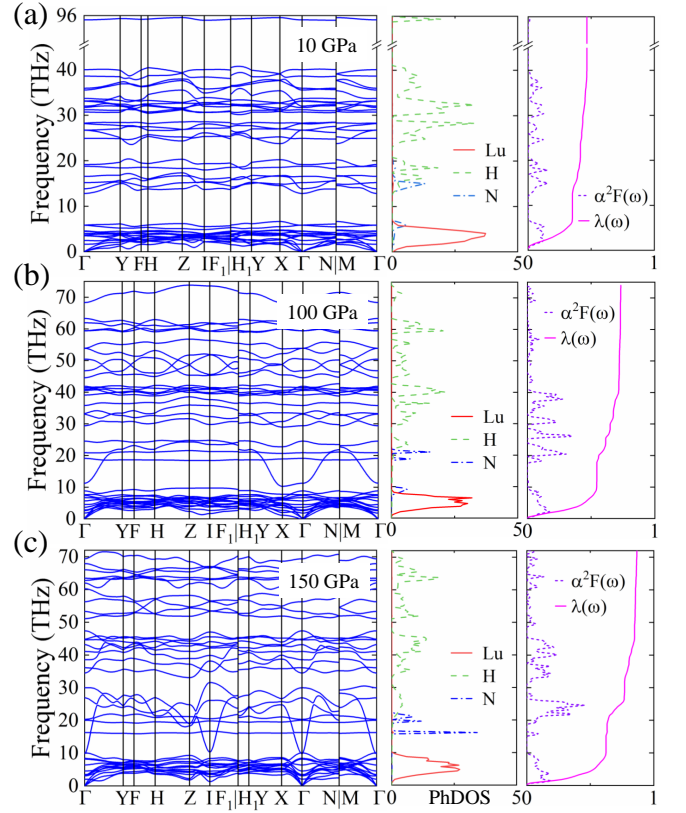


FIG. 4. The phonon spectra, projected PhDOS, $\alpha^2F(\omega)$, and $\lambda(\omega)$ of $\text{Lu}_4\text{H}_7\text{N}$ at (a) 10, (b) 100, and (c) 150 GPa.

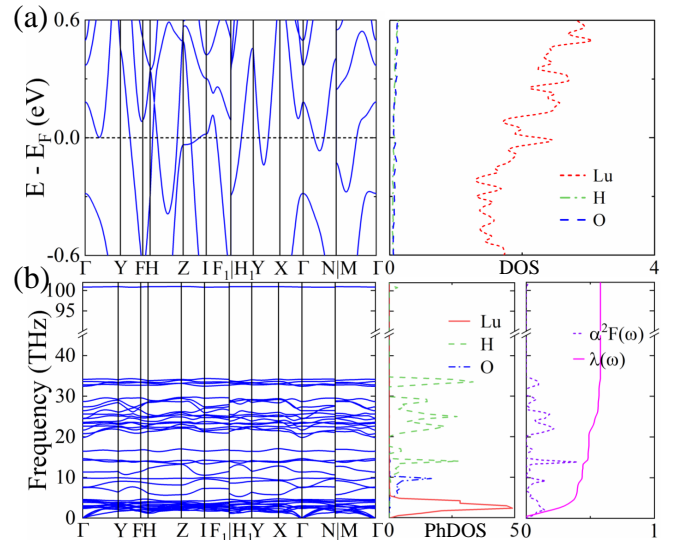


FIG. 5. (a) The electronic band structure, projected DOS, (b) phonon spectrum, projected PhDOS, $\alpha^2F(\omega)$, and $\lambda(\omega)$ of $\text{Lu}_4\text{H}_7\text{O}$.

remained dynamically stable, and the Tc reaches 1.892 K. However, with continued pressure increasing, the volume of Lu₄H₇N decreases, causing the N atoms to draw nearer to the surrounding Lu atoms which intensifies the repulsive forces, ultimately leading to dynamic instability. At an elevated pressure of 100 GPa, the positions of N atoms changed, resulting in the structure regaining its dynamical stability (for a detailed analysis, please refer to Sec. S3 of the Supplemental Materials [51]). Therefore, we postulate the existence of another structural form of Lu₄H₇N in the pressure range between 10 and 100 GPa. For the stable Lu₄H₇N structure above 100 GPa, we calculated its superconducting properties, as meticulously detailed in Table I. As the pressure increases, the electron DOS at the Fermi level gradually decreases, while ω_{log} steadily increases. As observed, the Tc of Lu₄H₇N reaches 11.721 K, with an enhanced EPC λ of 0.86 at 150 GPa. Fig. 4 presents the superconducting properties of Lu₄H₇N at 10, 100, and 150 GPa. Compared to Lu₄H₇N at ambient pressure and near-ambient pressure (10 GPa), it becomes evident that at pressures exceeding 100 GPa, the vibrations originating from Lu atoms, which constitute the primary contribution to λ , extend from the 0~5 THz range to 0~10 THz,, significantly increasing λ and driving an increase of Tc.

In addition, we replaced the N atom in Lu₄H₇N with a C or O atom to simulate hole or electron doping, respectively. Subsequently, we conducted thorough assessments of their superconducting properties, and proceeded to compare them with the well-known $Fm\bar{3}m$ LuH₂, as outlined in Table II. The electron DOS of LuH₂ and Lu₄H₇C at the Fermi level are much lower than that of Lu₄H₇N, weakening the EPC strength with a Tc less than 0.1 K. In stark contrast, as shown in Fig. 5, we observe a higher electron DOS at the Fermi level and PhDOS of Lu atoms in Lu₄H₇O, which serve as the primary source of λ , consequently enhancing the EPC strength and yielding an impressive Tc of 3.837 K.

IV. SUMMARY

To summarize, we predicted a new stable Lu-H-N compound Lu₄H₇N, which has a Tc of 1.044 K. Addition-

ally, Lu₄H₇N exhibits a strong Z₂ index and clear surface states near the Fermi level. The SOC opens several band gaps near the Fermi level, where large spin Berry curvatures exist and contribute significantly to the SHC of Lu₄H₇N. Furthermore, we found that the Tc of Lu₄H₇N can be enhanced to 11.721 K at 150 GPa. We also performed element substitution based on the Lu₄H₇N structure to simulate hole and electron doping and obtained two stable materials Lu₄H₇C and Lu₄H₇O with calculated Tc of 0.059 and 3.837 K, respectively. The change in Tc is primarily attributed to the modification of electronic DOS following doping. Our study reveals the co-existence of superconducting and topological properties within the Lu₄H₇N structure, making it valuable for advancing research on novel topological superconducting materials.

ACKNOWLEDGMENTS

This work is supported in part by the Innovation Program for Quantum Science and Technology (No. 2021ZD0301800), the National Key R&D Program of China (Grant No. 2018YFA0305800), the Strategic Priority Research Program of the Chinese Academy of Sciences (Grant No. XDB28000000), the National Natural Science Foundation of China (Grant No.11834014), and Beijing Municipal Science and Technology Commission (Grant No. Z118100004218001). B.G. is supported in part by the National Natural Science Foundation of China (Grant No. 12074378), the Chinese Academy of Sciences (Grant No. YSBR-030), the Strategic Priority Research Program of Chinese Academy of Sciences (Grant No. XDB33000000), and the Beijing Natural Science Foundation (Grant No. Z190011).

-
- [1] T. T. Heikkilä, M. Silaev, P. Virtanen, and F. S. Bergeret, *Prog. Surf. Sci.* **94**, 100540 (2019).
 - [2] A. Schilling, M. Cantoni, J. D. Guo, and H. R. Ott, *Nature* **363**, 56 (1993).
 - [3] J. Bardeen, L. N. Cooper, and J. R. Schrieffer, *Phys Rev* **108**, 1175 (1957).
 - [4] N. W. Ashcroft, *Phys. Rev. Lett.* **92**, 187002 (2004).
 - [5] D. Duan, Y. Liu, F. Tian, D. Li, X. Huang, Z. Zhao, H. Yu, B. Liu, W. Tian, and T. Cui, *Sci. Rep.* **4**, 6968 (2014).
 - [6] A. P. Drozdov, M. I. Erements, I. A. Troyan, V. Ksenofontov, and S. I. Shylin, *Nature* **525**, 73 (2015).
 - [7] F. Peng, Y. Sun, C. J. Pickard, R. J. Needs, Q. Wu, and Y. Ma, *Phys. Rev. Lett.* **119**, 107001 (2017).
 - [8] A. P. Drozdov, P. P. Kong, V. S. Minkov, S. P. Besedin, M. A. Kuzovnikov, S. Mozaffari, L. Balicas, F. F. Balakirev, D. E. Graf, V. B. Prakapenka, E. Greenberg, D. A. Knyazev, M. Tkacz, and M. I. Erements, *Nature* **569**, 528 (2019).
 - [9] I. Errea, F. Belli, L. Monacelli, A. Sanna, T. Koretsune, T. Tadano, R. Bianco, M. Calandra, R. Arita, F. Mauri,

- and J. A. Flores-Livas, *Nature* **578**, 66 (2020).
- [10] E. Zurek and T. Bi, *J. Chem. Phys.* **150**, 050901 (2019).
- [11] E. Zurek, *Comments Inorg. Chem.* **37**, 78 (2016).
- [12] G. Gao, L. Wang, M. Li, J. Zhang, R. T. Howie, E. Gregoryanz, V. V. Struzhkin, L. Wang, and J. S. Tse, *Materials Today Physics* **21**, 100546 (2021).
- [13] M. Somayazulu, M. Ahart, A. K. Mishra, Z. M. Geballe, M. Baldini, Y. Meng, V. V. Struzhkin, and R. J. Hemley, *Phys. Rev. Lett.* **122**, 027001 (2019).
- [14] N. Dasenbrock-Gammon, E. Snider, R. McBride, H. Pasan, D. Durkee, N. Khalvashi-Sutter, S. Munasinghe, S. E. Dissanayake, K. V. Lawler, A. Salamat, and R. P. Dias, *Nature* **615**, 244 (2023).
- [15] H. Song, Z. Zhang, T. Cui, C. J. Pickard, V. Z. Kresin, and D. Duan, *Chin. Phys. Lett.* **38**, 107401 (2021).
- [16] Z. Li, X. He, C. Zhang, K. Lu, B. Min, J. Zhang, S. Zhang, J. Zhao, L. Shi, Y. Peng, et al., *Science China Physics, Mechanics & Astronomy* **66**, 267411 (2023).
- [17] P. Shan, N. Wang, X. Zheng, Q. Qiu, Y. Peng, and J. Cheng, *Chin. Phys. Lett.* **40**, 046101 (2023).
- [18] X. Zhao, P. Shan, N. Wang, Y. Li, Y. Xu, and J. Cheng, *Science Bulletin* **68**, 883 (2023).
- [19] N. Wang, J. Hou, Z. Liu, P. Shan, C. Chai, S. Jin, X. Wang, Y. Long, Y. Liu, H. Zhang, X. Dong, and J. Cheng, (2023), [arXiv:2304.00558 \[cond-mat.supr-con\]](https://arxiv.org/abs/2304.00558).
- [20] X. Ming, Y.-J. Zhang, X. Zhu, Q. Li, C. He, Y. Liu, T. Huang, G. Liu, B. Zheng, H. Yang, J. Sun, X. Xi, and H.-H. Wen, *Nature* **620**, 72 (2023).
- [21] Y.-J. Zhang, X. Ming, Q. Li, X. Zhu, B. Zheng, Y. Liu, C. He, H. Yang, and H.-H. Wen, *Science China Physics, Mechanics & Astronomy* **66**, 287411 (2023).
- [22] X. Xing, C. Wang, L. Yu, J. Xu, C. Zhang, M. Zhang, S. Huang, X. Zhang, B. Yang, X. Chen, Y. Zhang, J. gang Guo, Z. Shi, Y. Ma, C. Chen, and X. Liu, (2023), [arXiv:2303.17587 \[cond-mat.supr-con\]](https://arxiv.org/abs/2303.17587).
- [23] S. Zhang, J. Bi, R. Zhang, P. Li, F. Qi, Z. Wei, and Y. Cao, *AIP Adv.* **13** (2023).
- [24] S. Cai, J. Guo, H. Shu, L. Yang, P. Wang, Y. Zhou, J. Zhao, J. Han, Q. Wu, W. Yang, T. Xiang, H. kwang Mao, and L. Sun, *Matter Radiat. at Extremes* **8**, 048001 (2023).
- [25] O. Moulding, S. Gallego-Parra, Y. Gao, P. Toulemonde, G. Garbarino, P. D. Rango, S. Pairis, P. Giroux, and M.-A. MÅfasson, (2023), [arXiv:2304.04310 \[cond-mat.supr-con\]](https://arxiv.org/abs/2304.04310).
- [26] P. Li, J. Bi, S. Zhang, R. Cai, G. Su, F. Qi, R. Zhang, Z. Wei, and Y. Cao, *Chin. Phys. Lett.* **40**, 087401 (2023).
- [27] Z. Liu, Y. Zhang, S. Huang, X. Ming, Q. Li, C. Pan, Y. Dai, X. Zhou, X. Zhu, H. Yan, and H.-H. Wen, (2023), [arXiv:2305.06103 \[cond-mat.supr-con\]](https://arxiv.org/abs/2305.06103).
- [28] M. Liu, X. Liu, J. Li, J. Liu, Y. Sun, X.-Q. Chen, and P. Liu, *Phys. Rev. B* **108**, L020102 (2023).
- [29] Z. Huo, D. Duan, T. Ma, Z. Zhang, Q. Jiang, D. An, H. Song, F. Tian, and T. Cui, *Matter Radiat. at Extremes* **8**, 038402 (2023).
- [30] F. Xie, T. Lu, Z. Yu, Y. Wang, Z. Wang, S. Meng, and M. Liu, *Chin. Phys. Lett.* **40**, 057401 (2023).
- [31] K. P. Hilleke, X. Wang, D. Luo, N. Geng, B. Wang, F. Belli, and E. Zurek, *Phys. Rev. B* **108**, 014511 (2023).
- [32] P. P. Ferreira, L. J. Conway, A. Cucciari, S. D. Cataldo, F. Giannessi, E. Kogler, L. T. F. Eleno, C. J. Pickard, C. Heil, and L. Boeri, *Nat. Commun.* **14**, 5367 (2023).
- [33] Y. Sun, F. Zhang, S. Wu, V. Antropov, and K.-M. Ho, *Phys. Rev. B* **108**, L020101 (2023).
- [34] R. Lucrezi, P. P. Ferreira, M. Aichhorn, and C. Heil, (2023), [arXiv:2304.06685 \[cond-mat.supr-con\]](https://arxiv.org/abs/2304.06685).
- [35] T. Lu, S. Meng, and M. Liu, (2023), [arXiv:2304.06726 \[cond-mat.supr-con\]](https://arxiv.org/abs/2304.06726).
- [36] S.-W. Kim, L. J. Conway, C. J. Pickard, G. L. Pascut, and B. Monserrat, (2023), [arXiv:2304.07326 \[cond-mat.supr-con\]](https://arxiv.org/abs/2304.07326).
- [37] Đ. Dangić, P. Garcia-Goiricelaya, Y.-W. Fang, J. Ibañez-Azpiroz, and I. Errea, *Phys. Rev. B* **108**, 064517 (2023).
- [38] Y. Wang, J. Lv, L. Zhu, and Y. Ma, *Phys. Rev. B* **82**, 094116 (2010).
- [39] G. Kresse and J. Furthmuller, *Phys. Rev. B* **54**, 11169 (1996).
- [40] A. A. Mostofi, J. R. Yates, G. Pizzi, Y.-S. Lee, I. Souza, D. Vanderbilt, and N. Marzari, *Comput. Phys. Commun.* **185**, 2309 (2014).
- [41] Q. Wu, S. Zhang, H.-F. Song, M. Troyer, and A. A. Soluyanov, *Comput. Phys. Commun.* **224**, 405 (2018).
- [42] P. Giannozzi, S. Baroni, N. Bonini, M. Calandra, R. Car, C. Cavazzoni, D. Ceresoli, G. L. Chiarotti, M. Cococcioni, I. Dabo, A. D. Corso, S. de Gironcoli, S. Fabris, G. Fratesi, R. Gebauer, U. Gerstmann, C. Gougoussis, A. Kokalj, M. Lazzeri, L. Martin-Samos, N. Marzari, F. Mauri, R. Mazzarello, S. Paolini, A. Pasquarello, L. Paulatto, C. Sbraccia, S. Scandolo, G. Scaluzero, A. P. Seitsonen, A. Smogunov, P. Umari, and R. M. Wentzcovitch, *J. Phys.: Condens. Matter* **21**, 395502 (2009).
- [43] P. E. Blochl, *Phys. Rev. B* **50**, 17953 (1994).
- [44] J. P. Perdew, K. Burke, and M. Ernzerhof, *Phys. Rev. Lett.* **77**, 3865 (1996).
- [45] G. Y. Guo, Y. Yao, and Q. Niu, *Phys. Rev. Lett.* **94**, 226601 (2005).
- [46] J. Sinova, D. Culcer, Q. Niu, N. A. Sinitsyn, T. Jungwirth, and A. H. MacDonald, *Phys. Rev. Lett.* **92**, 126603 (2004).
- [47] S. Baroni, S. de Gironcoli, A. D. Corso, and P. Giannozzi, *Rev. Mod. Phys.* **73**, 515 (2001).
- [48] M. Methfessel and A. T. Paxton, *Phys. Rev. B* **40**, 3616 (1989).
- [49] P. B. Allen and R. C. Dynes, *Phys. Rev. B* **12**, 905 (1975).
- [50] W. L. McMillan, *Phys. Rev.* **167**, 331 (1968).
- [51] See Supplemental Materials at [url] for crystal structure and instability of $Fm\bar{3}m$ LuH_3 and $\text{Lu}_4\text{H}_{11}\text{N}$, the spin Hall conductivity (SHC) of $\text{Lu}_4\text{H}_7\text{N}$, the pressure effects on $\text{Lu}_4\text{H}_7\text{N}$, and superconducting properties of $\text{Lu}_4\text{H}_7\text{C}$ which includes Refs. [14, 58].
- [52] A. Jain, S. P. Ong, G. Hautier, W. Chen, W. D. Richards, S. Dacek, S. Cholia, D. Gunter, D. Skinner, G. Ceder, and K. a. Persson, *APL Mater.* **1**, 011002 (2013).
- [53] R. Kieffer, P. Ettmayer, and S. Pajakoff, *Monatsh. Chem.* **103**, 1285 (1972).
- [54] W.-H. Dong, Y.-Y. Zhang, Y.-F. Zhang, J.-T. Sun, F. Liu, and S. Du, *npj Comput. Mater.* **8**, 185 (2022).
- [55] J.-Y. You, B. Gu, G. Su, and Y. P. Feng, *J. Am. Chem. Soc.* **144**, 5527 (2022).
- [56] X.-W. Yi, X.-Y. Ma, Z. Zhang, Z.-W. Liao, J.-Y. You, and G. Su, *Phys. Rev. B* **106**, L220505 (2022).
- [57] L. Fu and C. L. Kane, *Phys. Rev. B* **76**, 045302 (2007).
- [58] M. Seemann, D. Kodderitzsch, S. Wimmer, and H. Ebert, *Phys. Rev. B* **92**, 155138 (2015).
- [59] J.-Y. You, G. Su, and Y. P. Feng, *Natl. Sci. Rev.* , nwad114 (2023).